

One-pot Synthesis and Formation Mechanism of Prisms-built VO₂(M) with Hypersensitive Phase-transition Hysteresis^①

LI Xiong-Jian^② YANG Shui-Jin

(Hubei Key Laboratory of Pollutant Analysis & Reuse Technology, College of Chemistry and Chemical Engineering, Hubei Normal University, Huangshi 435002, China)

ABSTRACT Prisms-built VO₂(M) micro-nanostructures with narrow hysteresis width of 2.7 °C were successfully synthesized using V₂O₅-H₂C₂O₄-H₂O system by one-pot hydrothermal approach. The structure, composition, phase transition and optical properties were characterized by XRD, SEM, DSC, and variable-temperature UV-vis. The results revealed the prism had well-defined six facets and entire smooth surface with lengths of about 500 nm and thicknesses of around 100 nm. Several prisms were connected to each other through the apical growth. The prismatic VO₂(M) showed excellent phase transition and optical switching properties that would be beneficial for highly sensitive electrical/optical devices or other applications. The possible formation mechanism of prismatic VO₂(M) was proposed via time-dependent SEM images and XRD patterns. Furthermore, the influence of the amount of H₂O on the final product was discussed in detail.

Keywords: VO₂(M), optical properties, hysteresis width, one-pot synthesis;

DOI: 10.14102/j.cnki.0254-5861.2011-3086

1 INTRODUCTION

Vanadium dioxide (VO₂) as one of the most well-known binary compounds has various polymorphs, including VO₂(M) VO₂(B), VO₂(A), etc.^[1-4] Among these polymorphs, VO₂(M) has been paid much attention due to its interesting temperature-dependent optical and electrical properties induced by a fully reversible metal semiconductor transition between monoclinic VO₂(M) and tetragonal VO₂(R) at a critical temperature τ_c (68 °C for bulk VO₂)^[5, 6]. These properties give rise to a wide range of promising potential applications of VO₂(M) in intelligent energy conserving windows, electrical and optical devices, laser shield, flat panel displays, and so on^[7-11]. Among those, VO₂(M) applied as smart optical and electrical devices is identified as one of the most attractive applications. Thermal hysteresis (ΔT_c) named as the difference of phase transition temperature existing in the heating and cooling process is a key factor for evaluating sensitivity of smart optical and electrical devices^[12]. Generally, the wide ΔT_c does harm to the switching behavior and reduces the sensitivity of switching responses to temperature^[13]. In view of this, it is fascinating and significative to reduce the

ΔT_c of VO₂(M) usually depending on specific morphologies, sizes, dopants and synthetic methods.

In order to reduce the ΔT_c , numerous efforts have been concentrated on synthesizing VO₂(M) and doped VO₂(M) nanostructures using various technologies, including microwave irradiation method, sol-gel processes, RF sputtering, hydrothermal synthesis, physical/chemical vapor deposition and so forth^[5, 14]. However, comparative study of these references reveals that the ΔT_c for most reported VO₂(M) materials occurs in a broad temperature range of about 5~20 °C during reversible phase transition^[15]. For example, Li et al.^[16] reported the ΔT_c of VO₂(M) nanoparticles using interfacial defects and size effect approach exhibited an obvious hysteresis above 10 °C. Among doped VO₂(M) for reducing the ΔT_c , the dopant of Ti has been regarded as the first choice relative to other elements. Du et al.^[17] prepared a series of Ti-doped VO₂ films by polymer-assisted deposition and systematically studied their hysteresis; They found the ΔT_c reduced continuously from 38.2 to 3.5 °C with increasing the Ti content. Nevertheless, the doping process of VO₂(M) is complex and difficult to control, which would lead to the impurity and inhomogeneity of the final products.

Received 4 January 2021; accepted 8 February 2021 (ICSD 431051)

① This project was supported by the Hubei Provincial Department of Education (B2020129) and Scientific Research Foundation (HS2020RC021)

② Corresponding author. Li Xiong-Jian. E-mail: li_xiongjian@163.com

Although lots of studies have been reported for preparing pure VO₂(M) usually accompanied by subsequent annealing treatment at 450~700 °C^[18, 19], the direct formation of pure VO₂(M) using one-step approach has been rarely reported. Recently, Ji *et al.*^[20] reported one-pot hydrothermal synthesis of single crystal VO₂(M) in the V₂O₅-H₂C₂O₄-H₂O system by adding a proper amount of H₂SO₄ as pH adjustment agent. In addition, Chen *et al.*^[21] reported that pure VO₂(M) was difficult to synthesize and always mixed with VO₂(B). Therefore, the development of one-step synthesis of novel VO₂(M) to reduce the ΔT_c is highly desirable and challenging.

In this study, prism-built VO₂(M) micro-nanostructures were successfully synthesized using V₂O₅-H₂C₂O₄-H₂O system by one-pot hydrothermal approach without any additives. The prismatic VO₂(M) shows excellent phase transition with ΔT_c of 2.7 °C and optical switching properties that will be beneficial for highly sensitive smart optical and electrical devices or other applications. Furthermore, the influences of reaction time and amount of H₂O on the crystallized phase and morphologies of VO₂ were respectively discussed in detail. According to the experimental results, the possible formation mechanism of prismatic VO₂(M) was proposed.

2 EXPERIMENTAL

2.1 Synthesis of prismatic VO₂(M)

All of the reagents used in the experiments were analytically pure. In a typical synthesis, 1.460 g vanadium pentoxide (V₂O₅) and 2.020 g oxalic acid dihydrate (H₂C₂O₄·2H₂O) were dispersed into deionized water (62 mL) and stirred for 30 min at room temperature. Then, the suspension was transferred into an 80 mL stainless-steel autoclave and maintained at 260 °C for 48 h. After being accomplished, the autoclave was cooled down to room

temperature naturally. The precipitates were collected by centrifugation, washed with deionized water and ethanol several times and dried in the oven at 70 °C for more than 12 h.

2.2 Characterization

The as-prepared products were characterized by powder XRD using D8 X-ray diffractometer equipment with Cu-K α radiation, $\lambda = 1.54060$ Å. The morphologies were analyzed by scanning electron microscopy (SEM, Quanta 200). The phase transition temperature of the sample was measured by differential scanning calorimetry (DSC, DSC822^c, METTLER TOLEDO) with a heating ramp of 5 °C/min. Thermal gravimetric analysis (TGA) was performed on TG 209 F1. Optical properties of the samples were tested using UV-vis reflectance spectrum by adding a heater at the sample holder on a Shimadzu UV-3600 spectrophotometer using BaSO₄ as reference.

3 RESULTS AND DISCUSSION

Fig. 1a shows the XRD patterns of the obtained sample as well as the standard JPCDS plots of VO₂(M). By comparison, all diffraction peaks of the obtained products were readily indexed to the standard phase of VO₂(M) (JCPDS 43-1051) and no peaks of any other phases or impurities were detected. In addition, the strong diffraction peaks suggested a high crystallinity of VO₂(M). The morphologies of as-obtained sample were investigated by SEM (Figs. 1b and 1c). The panoramic view shown in Fig. 1b obviously displays that the obtained VO₂(M) consisted of a large quantity of uniform prisms. From the high-magnification SEM image (Fig. 1c), it can be clearly seen that these prisms possessed a well-defined six facets with entirely smooth surface, and had lengths of about 500 nm and thicknesses of around 100 nm. In addition, several prisms were connected to each other through the apical growth.

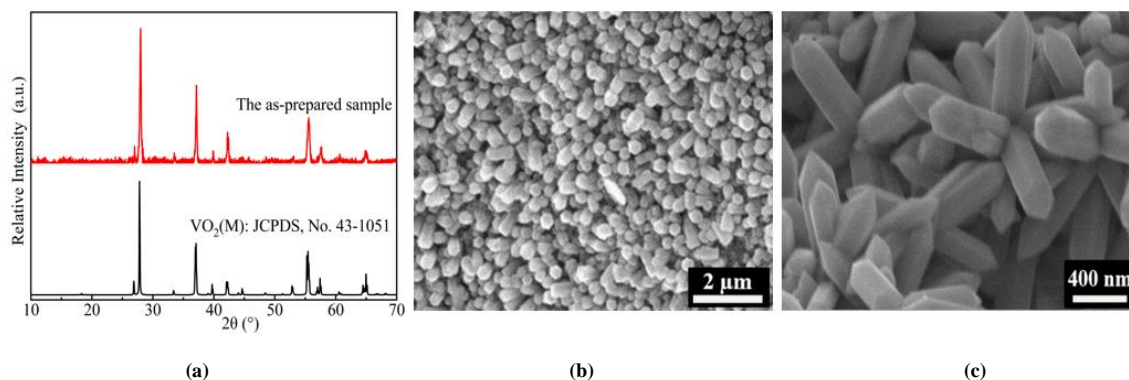


Fig. 1. (a) XRD patterns and (b, c) SEM images of the as-obtained VO₂(M)

To gain further understanding the formation process of prismatic $\text{VO}_2(\text{M})$ micro-nanostructures, time-dependent investigations were carried out by extracting products at different reaction stages. The synthetic processes were ceased at definite reaction periods of 6, 12, 24 and 36 h, and the as-obtained intermediate samples were thoroughly determined by XRD and SEM, as shown in Fig. 2. At the initial stage, the main diffraction peaks from the XRD pattern were indexed as monoclinic phase of $\text{VO}_2(\text{B})$ while some weak peaks were attributed to $\text{VO}_2(\text{M})$. It can be seen from the corresponding SEM image that the products were irregular nano-bulks with large variability in particle sizes. When the reaction was carried out for 12 h, the mixed crystalline phases mainly consisting of $\text{VO}_2(\text{B})$ and $\text{VO}_2(\text{M})$ were obtained, and lots of preformed prisms as well as a small number of nano-bulks were formed. After the reaction time was prolonged to 24 h, crystallized $\text{VO}_2(\text{M})$ became the

predominant phase and the incomplete prisms grew gradually. When the reaction time was extended to 36 h, the XRD pattern only displayed the diffraction peaks of $\text{VO}_2(\text{M})$ and good micro-nanostructures assembled by several prisms were formed through the apical growth. After the reaction was prolonged further to 48 h, high crystallinity of $\text{VO}_2(\text{M})$ with prisms-built micro-nanostructures was formed. On the basis of these experimental results, three steps, *i.e.*, nucleation, dissolution-recrystallization and subsequent growth, were proposed to explain the whole evolution process of prism-built $\text{VO}_2(\text{M})$ micro-nanostructures, as illustrated in Fig. 2f. In terms of the first step, metastable $\text{VO}_2(\text{B})$ phase was formed preferentially. With the reaction time going, the metastable phase dissolved into the solution system and the nucleation of $\text{VO}_2(\text{M})$ occurred and grew, and then evolved to prismatic assemblies in the process of Ostwald ripening growth^[13].

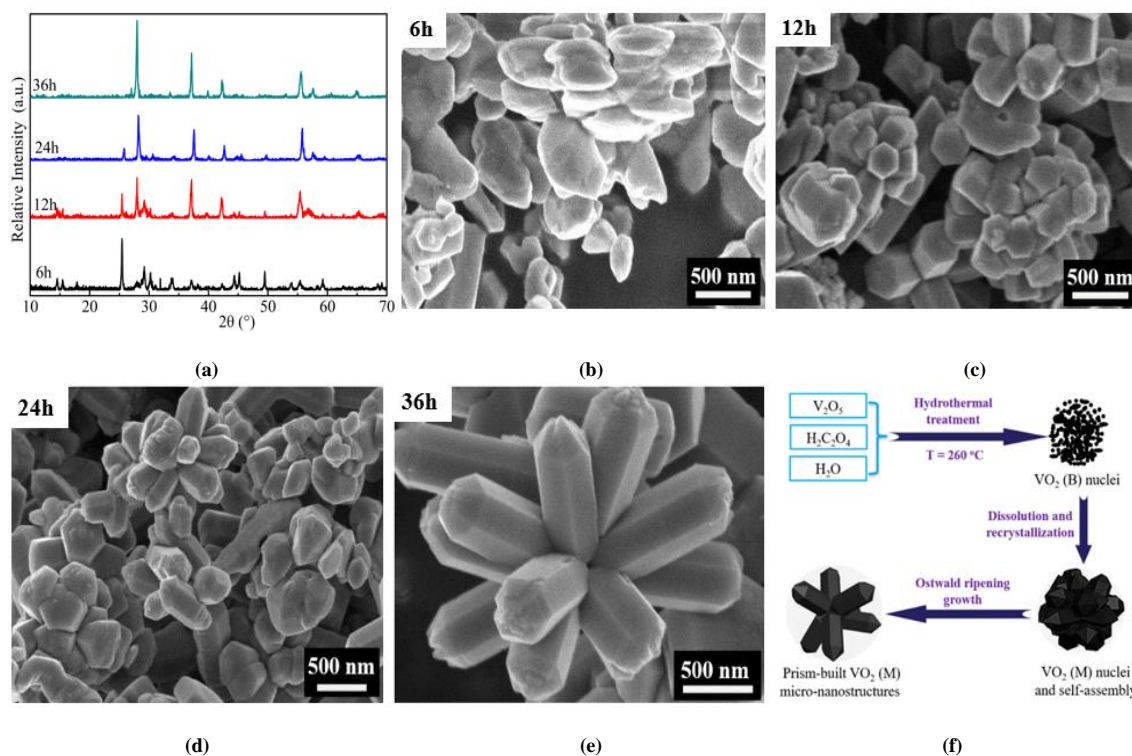


Fig. 2. (a) XRD patterns and (b~e) SEM images of the samples obtained at different growth stages, (f) formation mechanism of prism-built $\text{VO}_2(\text{M})$ micro-nanostructures

In addition, the amount of H_2O was found to be another important controlling factor on the phases of final products. Fig. 3a shows the corresponding XRD patterns of the samples produced with different amounts of H_2O . When the addition of H_2O was 50 mL, all diffraction peaks of samples were well indexed to the $\text{VO}_2(\text{A})$ phase (JCPDS 42-0876)^[15]. With H_2O addition increasing to 54 mL, some weak peaks attributed to

$\text{VO}_2(\text{M})$ appeared. As increasing H_2O to 60 mL, the phase suffered an important evolution, forming predominant $\text{VO}_2(\text{M})$ coupled with small amount of residual $\text{VO}_2(\text{A})$. Interestingly, with the continuous increase of H_2O to 68 mL, the peak intensities of $\text{VO}_2(\text{M})$ weakened and resulted in the formation of hydrated vanadium oxide phase, named, $\text{VO}_2(\text{M}) \cdot x\text{H}_2\text{O}$ ^[10,12]. Further increasing H_2O to 72 mL

resulted in the entire formation of VO₂(M) x H₂O. The phase and structure of the VO₂ (M) x H₂O were confirmed by thermal analysis of TG in flowing N₂ atmosphere as well as XRD, as shown in Figs. 3b and 3c, respectively. The TG plot exhibits a weight loss of 3.09% at the range of 200~450 °C

and x can be calculated as 0.147. After annealing at 500 °C for 2 h in flowing N₂ atmosphere, all diffraction peaks were indexed to VO₂(M), indicating the formation of crystallized VO₂(M) without any other parasitic phases.

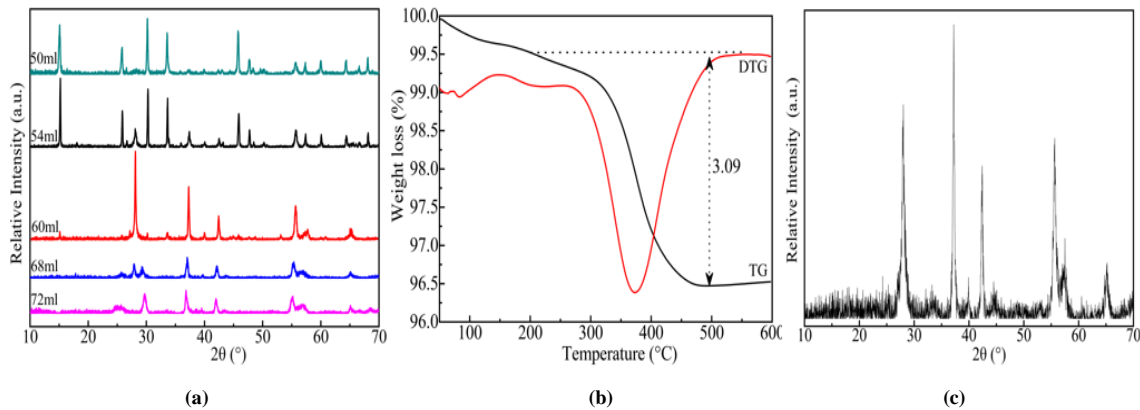


Fig. 3. (a) XRD patterns of the products synthesized from different amounts of H₂O at 260 °C for 48 h, (b) TG curve of VO₂(M) x H₂O in flowing N₂ atmosphere, (c) XRD pattern of as-obtained VO₂(M) x H₂O after heat treatment at 500 °C in flowing N₂ atmosphere

The reversible phase transition of VO₂(M) micro-nano-structures was investigated by DSC analysis. Fig. 4a shows the representative DSC curves of VO₂(M) with heating and cooling curves. The endothermic and exothermic peaks, implying the phase transition between VO₂(M) and VO₂(R), appeared at 56.5 and 53.8 °C, respectively. Furthermore, it displayed good cycle stability with thermal hysteresis width of 2.7 °C (ΔT_c). Table 1 shows the comparison of DSC results in the references and this work. The obtained prism-built VO₂(M) displayed much more narrowed ΔT_c compared to that reported in literatures. This indicates that the prism-built VO₂(M) showed high sensitivity to temperature. The showing narrow hysteresis width is due to the preferred crystallographic orientation which greatly

influences the width and switching temperature in the process of reversible phase transition^[22].

Variable-temperature UV-vis spectra were recorded to investigate the optical properties of obtained VO₂(M), as shown in Fig. 4b. It reveals that the prism-built VO₂(M) has good optical switching properties in visible region during phase transition while almost no changes in ultraviolet region. Above the transition temperature, the UV-vis curves at 80 and 120 °C coincided well with respect to no changes in phase transition. As VO₂(M) transforms to VO₂(R), the reflectivity in the 1500~2100 nm region decreased as a result of the formation of metal phase VO₂(R), leading to screening from the electrons delocalized at the surface of sample^[31]. In these regards, VO₂(M) can be applied as intelligent materials.

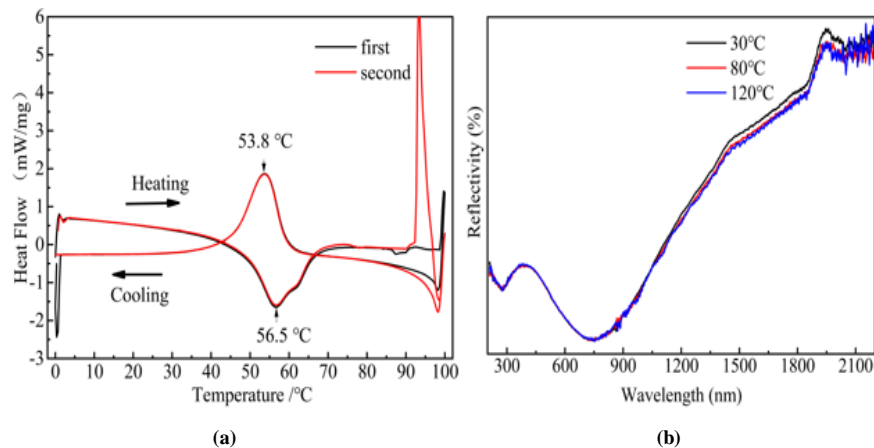


Fig. 4. (a) DSC curves with two cycles and (b) variable-temperature UV-vis spectra of as-obtained VO₂(M)

Table 1. Comparison of DSC Results in Literatures and This Work

$T_{\text{c-heating}} (^{\circ}\text{C})$	$T_{\text{c-cooling}} (^{\circ}\text{C})$	$\Delta T_{\text{c}} (^{\circ}\text{C})$	Ref.
67.1	59.4	7.7	[23]
78.6	60.6	18	[24]
68.6	55.2	13.3	[25]
47.6	41.0	6.6	[26]
65.9	62.5	3.4	
72.2	59.5	12.7	[27]
58	46	12	[28]
50	42	8	[29]
59	69	10	[30]
56.5	53.8	2.7	This work

4 CONCLUSION

In conclusion, prisms-built $\text{VO}_2(\text{M})$ micro-nanostructures with narrow hysteresis width of 2.7°C were successfully synthesized using $\text{V}_2\text{O}_5\text{-H}_2\text{C}_2\text{O}_4\text{-H}_2\text{O}$ system by one-pot hydrothermal approach. The reaction time and amount of H_2O were the key factors for the synthesis of $\text{VO}_2(\text{M})$. The prepared $\text{VO}_2(\text{M})$ consisted of numerous prisms connected to

each other through the apical growth. The prisms had well-defined six facets and entire smooth surface with lengths of about 500 nm and thicknesses of around 100 nm. The prismatic $\text{VO}_2(\text{M})$ showed excellent phase transition and optical switching properties that would be beneficial for highly sensitive electrical/optical devices or other applications.

REFERENCES

- (1) Yu, W.; Li, S.; Huang, C. Phase evolution and crystal growth of VO_2 nanostructures under hydrothermal reactions. *RSC Adv.* **2016**, 6, 7113–7120.
- (2) Zhang, L.; Xia, F.; Song, Z.; Webster, N. A. S.; Luo, H.; Gao, Y. Synthesis and formation mechanism of VO_2 (A) nanoplates with intrinsic peroxidase-like activity. *RSC Adv.* **2015**, 5, 61371–61379.
- (3) Cao, C.; Gao, Y.; Luo, H. Pure single-crystal rutile vanadium dioxide powders: synthesis, mechanism and phase-transformation property. *J. Phys. Chem. C* **2008**, 112, 18810–18814.
- (4) Qu, B. Y.; Liu, L.; Xie, Y.; Pan, B. C. Theoretical study of the new compound VO_2 (D). *Phys. Lett. A* **2011**, 375, 3474–3477.
- (5) Zhang, H.; Xiao, X.; Lu, X.; Chai, G.; Sun, Y.; Zhan, Y.; Xu, G. A cost-effective method to fabricate $\text{VO}_2(\text{M})$ nanoparticles and films with excellent thermochromic properties. *J. Alloys Compd.* **2015**, 636, 106–112.
- (6) Wang, Y.; Chen, C. Facile growth of thermochromic VO_2 nanostructures with greatly varied phases and morphologies. *Inorg. Chem.* **2013**, 52, 2550–2555.
- (7) Li, M.; Magdassi, S.; Gao, Y.; Long, Y. Hydrothermal synthesis of VO_2 polymorphs: advantages, challenges and prospects for the application of energy efficient smart windows. *Small* **2017**, 13, 1701147.
- (8) Zhang, Y.; Li, W.; Fan, M.; Zhang, F.; Zhang, J.; Liu, X.; Zhang, H.; Huang, C.; Li, H. Preparation of W- and Mo-doped $\text{VO}_2(\text{M})$ by ethanol reduction of peroxovanadium complexes and their phase transition and optical switching properties. *J. Alloys Compd.* **2012**, 544, 30–36.
- (9) Liang, S.; Shi, Q.; Zhu, H.; Peng, B.; Huang, W. One-step hydrothermal synthesis of W- doped $\text{VO}_2(\text{M})$ nanorods with a tunable phase-transition temperature for infrared smart windows. *ACS Omega* **2016**, 1, 1139–1148.
- (10) Powell, M. J.; Quesada-Cabrera, R.; Taylor, A.; Teixeira, D.; Papakonstantinou, I.; Palgrave, R. G.; Sankar, G.; Parkin, I. P. Intelligent multifunctional $\text{VO}_2/\text{SiO}_2/\text{TiO}_2$ coatings for self-cleaning, energy-saving window panels. *Chem. Mater.* **2016**, 28, 1369–1376.
- (11) Liu, K.; Cheng, C.; Suh, J.; Tang-Kong, R.; Fu, D. Y.; Lee, S.; Zhou, J.; Chua, L. O.; Wu, J. Q. Powerful, multifunctional torsional micromuscles activated by phase transition. *Adv. Mater.* **2014**, 26, 1746–1750.
- (12) Chen, S.; Liu, J.; Wang, L.; Luo, H.; Gao, Y. Unraveling mechanism on reducing thermal hysteresis width of VO_2 by Ti doping: a joint experimental and theoretical study. *J. Phys. Chem. C* **2014**, 118, 18938–18944.
- (13) Li, X.; Zhang, S.; Yang, L.; Li, X.; Chen, J.; Huang, C. A convenient way to reduce the hysteresis width of VO_2 (M) nanomaterials. *New J. Chem.* **2017**, 41, 15260–15267.
- (14) Guo, B.; Chen, L.; Shi, S.; Ishaq, A.; Wan, D.; Chen, Z.; Zhang, L.; Luo, H.; Gao, Y. Low temperature fabrication of thermochromic VO_2 thin films

- by low-pressure chemical vapor deposition. *RSC Adv.* **2017**, 7, 10798–10805.
- (15) Li, X.; Yang, L.; Zhang, S.; Li, X.; Chen, J.; Huang, C. VO₂(M) with narrow hysteresis width from a new metastable phase of crystallized VO₂(M)·0.25H₂O. *Mater. Lett.* **2018**, 211, 308–311.
- (16) Li, M.; Wu, X.; Li, L.; Wang, Y.; Li, D.; Pan, J.; Li, S.; Sun, L.; Li, G. Defect-mediated phase transition temperature of VO₂ (M) nanoparticles with excellent thermochromic performance and low threshold voltage. *J. Mater. Chem. A* **2014**, 2, 4520–4523.
- (17) Du, J.; Gao, Y.; Luo, H.; Kang, L.; Zhang, Z.; Chen, Z.; Cao, C. Significant changes in phase-transition hysteresis for Ti-doped VO₂ films prepared by polymer-assisted deposition. *Sol. Energy Mater. Sol. Cells* **2011**, 95, 469–475.
- (18) Zhang, Y.; Huang, Y.; Zhang, J.; Wu, W.; Niu, F.; Zhong, Y.; Liu, X.; Liu, X.; Huang, C. Facile synthesis, phase transition, optical switching and oxidation resistance properties of belt-like VO₂ (A) and VO₂ (M) with a rectangular cross section. *Mater. Res. Bull.* **2012**, 47, 1978–1986.
- (19) Ma, Y.; Zhou, H.; Zhu, J.; Ji, S.; Bao, S.; Li, R.; Jin, P. Synthesis of flake-like VO₂(M) by annealing a novel (NH₄)_{0.6}V₂O₅ phase and its thermochromic characterization. *Ceram. Int.* **2016**, 42, 16382–16386.
- (20) Ji, S.; Zhao, Y.; Zhang, F.; Jin, P. Direct formation of single crystal VO₂(R) nanorods by one-step hydrothermal treatment. *J. Cryst. Growth* **2010**, 312, 282–286.
- (21) Chen, R.; Miao, L.; Liu, C.; Zhou, J.; Cheng, H.; Asaka, T.; Iwamoto, Y.; Tanemura, S. Shape-controlled synthesis and influence of W doping and oxygen nonstoichiometry on the phase transition of VO₂. *Sci. Rep-UK* **2015**, 5, 14087–14099.
- (22) Binions, R.; Hyett, G.; Piccirillo, C.; Parkin, I. P. Doped and un-doped vanadium dioxide thin films prepared by atmospheric pressure chemical vapour deposition from vanadyl acetylacetonate and tungsten hexachloride: the effects of thickness and crystallographic orientation on thermochromic properties. *J. Mater. Chem.* **2007**, 17, 4652–4660.
- (23) Liu, L.; Cao, F.; Yao, T.; Xu, Y.; Zhou, M.; Qu, B.; Pan, B.; Wu, C.; Wei, S.; Xie, Y. New-phase VO₂ micro/nanostructures: investigation of phase transformation and magnetic property. *New J. Chem.* **2012**, 36, 619–625.
- (24) Li, M.; Wu, X.; Li, L.; Wang, Y.; Li, D.; Pan, J.; Li, S.; Sun, L.; Li, G. Defect-mediated phase transition temperature of VO₂ (M) nanoparticles with excellent thermochromic performance and low threshold voltage. *J. Mater. Chem. A* **2014**, 2, 4520–4523.
- (25) Zhang, K. F.; Zhang, G. Q.; Liu, X.; Su, Z.; Li, H. Large scale hydrothermal synthesis and electrochemistry of ammonium vanadium bronze nanobelts. *J. Power Sources* **2006**, 157, 528–532.
- (26) Song, Z.; Zhang, L.; Xia, F.; Webster, N. A. S.; Song, J.; Liu, B.; Luo, H.; Gao, Y. Controllable synthesis of VO₂(D) and their conversion to VO₂(M) nanostructures with thermochromic phase transition properties. *Inorg. Chem. Front.* **2016**, 3, 1035–1042.
- (27) Zhang, Y.; Fan, M.; Wu, W.; Hu, L.; Zhang, J.; Mao, Y.; Huang, C.; Liu, X. A novel route to fabricate belt-like VO₂(M)@C core-shell structured composite and its phase transition properties. *Mater. Lett.* **2012**, 71, 127–130.
- (28) Zhang, Y.; Zhang, J.; Zhang, X.; Mo, S.; Wu, W.; Niu, F.; Zhong, Y.; Liu, X.; Huang, C.; Liu, X. Direct preparation and formation mechanism of belt-like doped VO₂(M) with rectangular cross sections by one-step hydrothermal route and their phase transition and optical switching properties. *J. Alloys Compd.* **2013**, 570, 104–113.
- (29) Zhang, Y.; Zhang, X.; Huang, Y.; Huang, C.; Niu, F.; Meng, C.; Tan, X. One-step hydrothermal conversion of VO₂(B) into W-doped VO₂(M) and its phase transition and optical switching properties. *Solid State Commun.* **2014**, 180, 24–27.
- (30) Chen, Y.; Ma, S.; Li, X.; Zhao, X.; Cheng, X.; Liu, J. Preparation and microwave absorption properties of microsheets VO₂(M). *J. Alloys Compd.* **2019**, 791, 307–315.
- (31) Guinneton, F.; Sauques, L.; Valmalette, J. C.; Cros, F.; Gavarrí, J. R. Comparative study between nanocrystalline powder and thin film of vanadium dioxide VO₂: electrical and infrared properties. *J. Phys. Chem. Solids* **2001**, 62, 1229–1238.